Ferric leaching of the sphalerite contained in a bulk concentrate: kinetic study

Juan Lorenzo-Tallafigo, Nieves Iglesias-Gonzalez, Rafael Romero, Alfonso Mazuelos, Francisco Carranza

Abstract

A novel process for the integral treatment of polymetallic sulphide ores is proposed. The process consists of a global flotation, two stages of ferric leaching, the first stage dissolves the sphalerite and the rest of secondary sulphides, and the second dissolves the chalcopyrite with a silver catalyst, and finally a brine leaching to recover lead and silver (added as catalyst). The proposed process offers several advantages comparing to traditional pyrometallurgical techniques. This study is focused on the sphalerite dissolution with ferric sulphate, as the first stage of the treatment of Cu-Zn-Pb concentrates. The ferric ion concentration, the temperature and the particle size have an important role in the sphalerite oxidation. However, the initial sulphuric acid, ferrous ion and sulphate ion concentrations have no influence in the process rate. The formation of an elemental non-porous layer of sulphur along the reaction hinders the ferric ion transport to the sphalerite surface. Two kinetics regimes are proposed, in the beginning the chemical reaction is the rate controlling step, and, at 30% Zn extraction, the rate controlling step changes to diffusion through a non-porous film of elemental sulphur. The activation energy obtained for the chemical reaction has a value of 51.3 kJ/mol, and the apparent activation energy in the diffusional stage is the 47.7 kJ/mol. The reaction order with respect ferric ion is 0.26 and the reaction rate is proportional to the zinc sulphide amount in the first stage. The behaviour of sphalerite, contained in a bulk concentrate, is similar to the pure sphalerite or the sphalerite contained in a differential concentrate.

Keywords

Ferric leaching

Kinetics

Sphalerite

Bulk concentrate

Polymetallic sulphide

1. Introduction

Almost all of the world's primary zinc production is derived from the treatment of sulphide concentrate, obtained through differential flotation, in which sphalerite is the dominant zinc mineral (Dutrizac, 2006). The *roast-leach-Electrowinning Process* (R-L-E) is currently responsible for more than 85% of the total zinc production (Souza et al., 2007b). This process has several troubles, such as the restrictions to treat sphalerite concentrate with silica, calcium, copper and iron, the emissions of SO_2 and marketing of sulphuric acid (Deller, 2005). Several processes have been studied, in the last years, to extract Zn from differential concentrates, such as atmospheric pressure leaching (Salmi et al., 2010; Souza et al., 2007a; Babu et al, 2002), bioleaching (Haghshenas et al., 2012) or heap-Bioleaching (Lizama et al., 2003).

Most of these processes need a previous concentration of zinc sulphide through a differential flotation. Differential flotation has several disadvantages regarding global flotation, where a concentrate of all non-ferrous metals is obtained, such as a lower recuperation of non-ferrous metals, high content of impurities in the concentrates or a greater grinding energetic consumption (Carranza, 1985; Majima, 1969; Tipre et al., 1999; Carranza et al., 1993). Global concentrates must be treated through hydrometallurgical processes because these processes offer a greater versatility to extract the valuable metals from different ores, and low-grade concentrates, and are more environmentally friendly than pyrometallurgical processes (Córdoba et al., 2008; Carranza et al., 1997b; Conic et al., 2014). Zinc, and the rest of metals, can be extracted from global concentrates through bacterial leaching (Tipre and Dave, 2004; Conic et al, 2014; Gómez et al., 1999 and Gómez et al., 1997), pressure leaching with O_2 (Xu et al., 2011 and Xu et al., 2016) and atmospheric pressure leaching with ferric ion, as ferric sulphate, only studied with Cu-Zn concentrates (Carranza et al., 1997a and Palencia et al., 1990). Ferric chloride reaches higher reaction rates, but this leaching agent increases industrial costs due to equipment corrosion. Conversely, ferric sulphate is a cheap and efficient oxidant agent to dissolve non-ferrous metals and can be regenerated by bio-oxidation (Mazuelos et al., 2000; Carranza et al., 1993; Palencia et al., 1990; Gómez et al., 1997; Dutrizac et al., 2003; Aydogan et al., 2005).

Global concentrates obtained from polymetallic sulphides of the Iberian Pyritic Belt (IPB) are composed, basically, of sphalerite, chalcopyrite, galena and pyrite, as majority sulphide (Ortega and Bonilla, 1983). Fig. 1 shows some possibilities to benefit these polymetallic sulphides: the traditional processes, by pyrometallurgical methods, and the

hydrometallurgical processes. The hydrometallurgical treatment, shown in Fig. 1, of bulk concentrates (Cu, Zn and Pb) is proposed as an integral treatment where Cu, Zn and Pb are recuperated from one sole concentrate and through a unique process. This hydrometallurgical plant can be located within the mining facilities, changing the production model of concentrates sales to production and sales of metals.

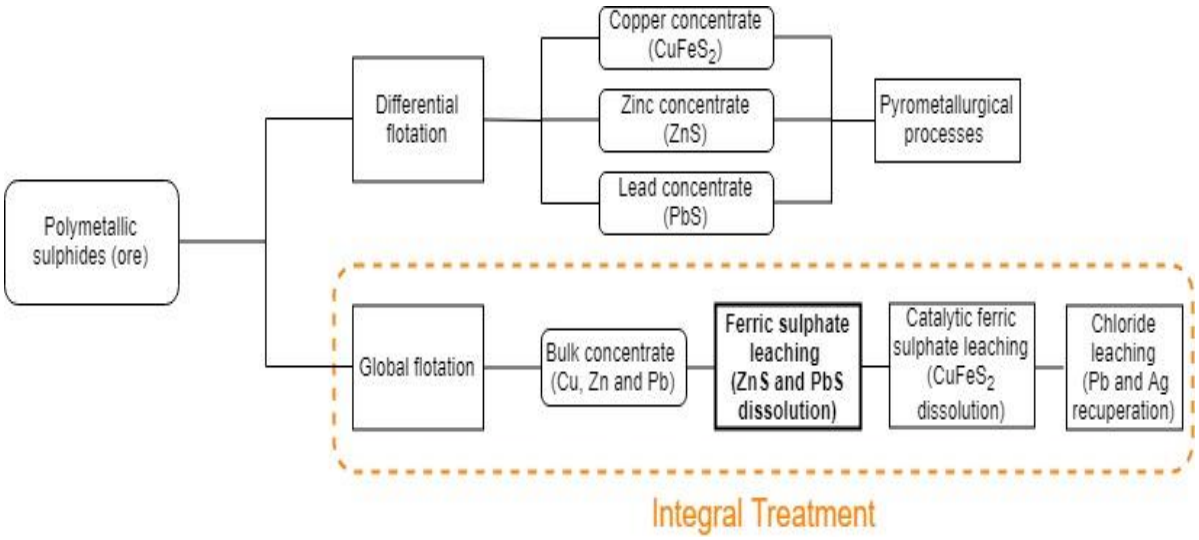

Figure 1: Diagram of hydrometallurgical process vs. traditional processes to polymetallic sulphides exploitation.

From a conceptual point of view (see Fig. 1), the ferric sulphate leaching, to benefit a concentrate that contains Zn, Cu, Pb and Ag, could consist of a first stage where zinc sulphide, and the rest of secondary sulphides, are dissolved and a catalytic second stage in presence of silver salts, where chalcopyrite is oxidised. First stage is necessary because silver catalyst is not selective and passives the dissolution of the rest of non-ferrous sulphides. Silver and lead are extracted through a chloride leaching of solid residue (Palencia et al., 1998 and Bahram and Javad, 2011). In this stage, the silver added as catalyst is recovered (Carranza et al., 2004; Carranza et al., 1997a; Barriga Mateos et al., 1993). Chemical reactions in the ferric leaching of a global concentrate, containing FeS_2, $Zn_xFe_{1-x}S$, CuS, Cu_2S, PbS and $CuFeS_2$ are r1-r5:

$$FeS_2 + 14Fe^{3+} + 8H_2O \rightarrow 15Fe^{2+} + 16H^+ + 2SO_4^{2-} \quad (r1)$$

$$Cu_2S + 2Fe^{3+} \rightarrow CuS + Cu^{2+} + 2Fe^{2+} \quad (r2)$$

$$CuS + 2Fe^{3+} \rightarrow Cu^{2+} + 2Fe^{2+} + S^0 \quad (r3)$$

$$Zn_xFe_{1-x}S + 2Fe^{3+} \rightarrow xZn^{2+} + 3\text{-}xFe^{2+} + S^0 \quad (r4)$$

$PbS + 2Fe^{3+} \rightarrow Pb^{2+} + 2Fe^{2+} + S^0$ (r5)

In this medium, chalcopyrite is passivated due to the formation of a metal deficient film according to r6 (Ghahremaninezhad et al., 2015).

$CuFeS_2 \rightarrow Cu_{1-x}Fe_{1-y}S_2 + yFe^{2+} + xCu^{2+} + 2(x+y)e- \; ; \; y > x$ (r6)

Various secondary reactions take place, as the lead sulphate precipitation (r7) or the possibility to regenerate the leaching agent (r8), which can be catalysed by bacteria. A possible mechanism to sphalerite dissolution found in literature, where sulphuric acid and ferric ion concentrations affect the reaction rate, is given by r9-r10.

$Pb^{2+} + SO_4^{2-} \rightarrow PbSO_4$ (r7)

$2Fe^{2+} + 1/2O_2 + 2H^+ \rightarrow 2Fe^{3+} + H_2O$ (r8)

$ZnS + 2H^+ \rightarrow Zn^{2+} + H_2S$ (r9)

$H_2S + 2Fe^{3+} \rightarrow 2Fe^{2+} + 2H^+ + S^0$ (r10)

Sphalerite leaching reaction with ferric ion has been extensively studied in zinc sulphide concentrate and natural crystals of pure sphalerite (Dutrizac, 2006; Salmi et al., 2010; Palencia and Dutrizac, 1991; Souza et al., 2007a; Crundwell, 1987b; Dutrizac and Macdonald, 1978; Estrada-de los Santos et al., 2016; Chang et al., 1994; Weisener et al., 2003; Da Silva, 2004). These studies can be summarized in the following points:

- Fe content in sphalerite structure has a great influence on sphalerite leaching reaction rate. The increment of iron impurities in sphalerite enhances the sphalerite leaching rate, decreasing the activation energy. An activation energy of 70 kJ/mol was observed for a sphalerite with 0.04% wt of iron, instead, for a sphalerite with 12.5% wt of iron the activation energy was around of 40 kJ/mol (Palencia and Dutrizac, 1991; Crundwell, 1988).
- The presence of other sulphides can change the reactivity of sphalerite due to the formation of galvanic couples. Sulphides with a higher rest potential than sphalerite enhance the sphalerite dissolution, and the sulphides with a lower rest potential, such as galena and chalcocite, decrease the sphalerite leaching rate (Mizoguchi and Habashi, 1983; Lo et al., 1985; Elsherief, 1994; Estrada de los Santos et al., 2016; Da Silva et al., 2003; Mehta and Murr, 1982).

- Many authors have found a great influence of sulphuric acid concentration on sphalerite leaching rate, according to r9-10, where H_2S is formed as a reaction intermediate (Dutrizac, 2006; Dutrizac and Macdonald, 1978; Souza et al., 2007a; Verbaan and Crundwell, 1986). Dutrizac (2006) observed that the reaction rate depends on sulphuric acid concentration only when this concentration is higher than 0.1M. However, other authors found no influence of sulphuric acid on sphalerite oxidation rate (Salmi et al., 2010; Santos et al., 2010).
- The rate controlling step is a reason for discrepancy between authors. Some authors have observed that chemical reaction is the rate controlling step (Dutrizac, 2006; Palencia and Dutrizac, 1991; Markus et al., 2004; Salmi et al., 2010). While, in other cases, the rate controlling step is the diffusion through a passive film (Dutrizac and Macdonald, 1978; Palencia et al., 1990; Lampimen et al., 2015). Also, other authors have found a mixed control, where at the beginning of the reaction the rate controlling step is the chemical reaction and later the controlling step changes to the diffusion through a non-porous film (Souza et al., 2007a; Lochmann and Pedlik, 1995; Weisener et al., 2003).

From the above, the sphalerite behaviour has a great dependence on the ore nature and the treatment performed. Unlike samples (high-grade or pure sphalerite) used in previous studies, bulk concentrates are low-grade in copper, zinc and lead, can present galvanic-couples formation (due to the presence of different sulphide phases) and the leaching behaviour of these sulphides can be affected by reaction products formed along dissolution reactions, such as $PbSO_4$, or by the nature of passivating film formed (Estrada et al., 2016 and Da Silva et al., 2003). Also, physical hindrances can be found due to occlusion of different mineral phases in others. For these reasons it is of great importance to study the sphalerite dissolution from a bulk concentrate to optimise the first stage of the above proposed process.

The exhaustive knowledge of kinetic and thermodynamic aspects of these solid-liquid reactions is crucial to the optimisation of processes and industrial plants (Grénman et al., 2011; Habashi, 2005). The knowledge of reaction kinetic can be performed by means of the adjustment of experimental data to different models, these models are based on ideal cases, and on the solid characterisation, such as the specific surface area measurement. Table 1 shows different kinetic equations for solid particles dissolution (Levenspiel, 2004, Dickinson and Heal, 1999; Órfao and Martins, 2002). In previous studies models

R3 and D4 have been the most used to explain the sphalerite dissolution, but other kinetic equations, shown in Table 1, can be useful to describe this reaction as well. For a more complete review of the kinetic models see Dickinson and Heal (1999), Órfao and Martins (2002), Levenspiel (2004), Brown et al (1980) and Khawam and Flanagan (2006).

Table 1: Equations of different kinetic models for solid particles dissolution. Being k the rate constant, α the reaction conversion and t the reaction time (adapted from Dickinson and Heal, 1999).

Notation	$\mathbf{g(\alpha) = kt}$	**Type of model**
F1	$-\ln(1-\alpha) = kt$	First-order kinetics
F3/2	$(1-\alpha)^{-1/2} - 1 = kt$	Three-halves-order kinetics
F2	$(1-\alpha)^{-1} = kt$	Second-order kinetics
R2	$1-(1-\alpha)^{1/2} = kt$	One-half-order-kinetics; 2-D advance of the reaction interface
R3	$1-(1-\alpha)^{1/3} = kt$	Two-thirds-order kinetics; 3-D advance of the reaction interface
R4	$1-(1-\alpha)^{2/3} = kt$	One-thirds-order-kinetics; film diffusion
D3	$\left[1-(1-\alpha)^{1/3}\right]^2 = kt$	Jander; 3-D
D4	$1-\frac{2}{3}\alpha-(1-\alpha)^{2/3} = kt$	Crank-Ginstling and Brounshtein
D5	$\left\lfloor\frac{1}{(1-\alpha)^{1/3}}-1\right\rfloor^2 = kt$	Zhuravlev, Lesokhin and Tempelman
D6	$\left[(1+\alpha)^{1/3}-1\right]^2 = kt$	Anti-Jander (3-D)
D8	$\left[1-(1-\alpha)^{1/2}\right]^2 = kt$	Jander; cylindrical diffusion
D10	$\frac{1}{(1-\alpha)^{1/3}}-1 = kt$	Dickinson and Heal

This work is part of a research project for the integral treatment of bulk concentrates through the proposed hydrometallurgical process and aims the study of the sphalerite dissolution with ferric sulphate as the first stage of this process. This work consists of two sections: the first is an exhaustive study of the effect of variables that can affect the process rate (Temperature, pulp density, particle size, elemental sulphur film and the concentrations of ferric ion, sulphuric acid, ferrous ion and sulphate ion), and the second is the evaluation of the sphalerite dissolution kinetic by the application of several models.

2. Materials and methods

2.1 Bulk concentrate

The concentrate used in this work is a bulk concentrate of polymetallic sulphide ore from Cobre las Cruces Mine (Spain). The concentrate was separated in two fractions: one higher than 25 μm (Cl-A) and other lower than 25 μm (Cl-B), also, a part of the bulk concentrate was reground (Cl-C). The chemical composition of the bulk concentrate and the different samples is shown in Table 2. The chemical composition of Cl-C is the same as that of bulk concentrate. Chemical composition is similar in all cases, having a high non-ferrous metal concentration the sample with higher particle size (Cl-A). Table 3 shows the specific surface area (σ), measured by nitrogen physisorption, the shape factor (a), and the mean diameter (d_0) and D80, obtained from laser diffraction, Beckman Coulter LS 13-320-MW model, for the different samples. Also, Fig. 2 shows the differential granulometric curves, where is observed that Cl-A differs from other samples. σ is higher than the surface area corresponding to a spherical geometry in all cases, and the porosity raise up as the particle sizes increases. Besides, specific surface area has not a direct relationship to particle size, it also was observed by Souza et al. (2007a). Fig. 3 shows the X-ray pattern where the following mineral phases: pyrite, sphalerite, chalcopyrite and galena, are identified. Fig. 4 shows two micrographs where chalcopyrite, pyrite and sphalerite are identified, part of sphalerite is encapsulated in the pyrite particles. The concentrate characterization shows a low-grade sulphide in target metals, this is proper in a global flotation process. Sphalerite is associated with other sulphides (pyrite, galena and chalcopyrite) that could affect the sphalerite dissolution behaviour.

Table 2: Chemical composition and sphalerite percentage of different samples.

Sample	**Fe (%)**	**Zn (%)**	**Pb (%)**	**Cu (%)**	**Ag (ppm)**	**Sphalerite (%)**
Bulk concentrate	34.60	8.47	3.98	4.92	116	12.43
Cl-A	36.90	10.09	4.90	5.54	173	14.81
Cl-B	32.50	6.99	3.79	4.76	72	10.26

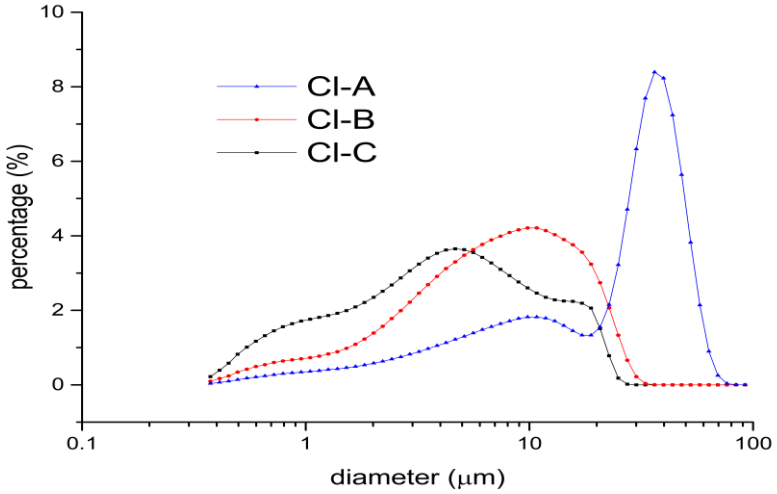

Figure 2: Differential granulometric curves of samples used in this work.

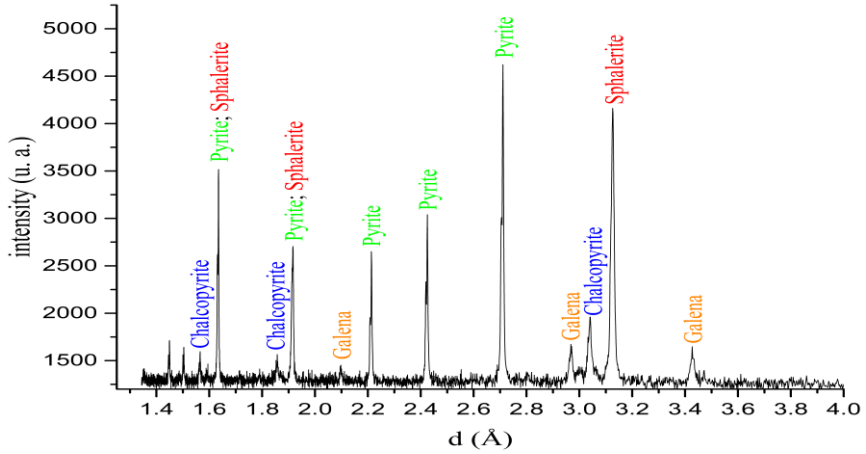

Figure 3: X-ray pattern of global concentrate (kα1-Cu radiation, wave length (λ) = 0.1542 nm and 2θ from 3 to 70º).

Table 3: Sample Characterisation through physisorption measurement with N_2 and laser diffraction.

Concentrate	BET Surface area (m^2/g)	Micropore area (m^2/g)	D80 (μm)	d_0 (μm)	Shape factor (a)
Cl-A	2.025	0.241	43.7	27.7	127.3
Cl-B	1.884	0.117	14.8	9.1	38.9
Cl-C	3.760	0.030	10.2	6.2	52.9

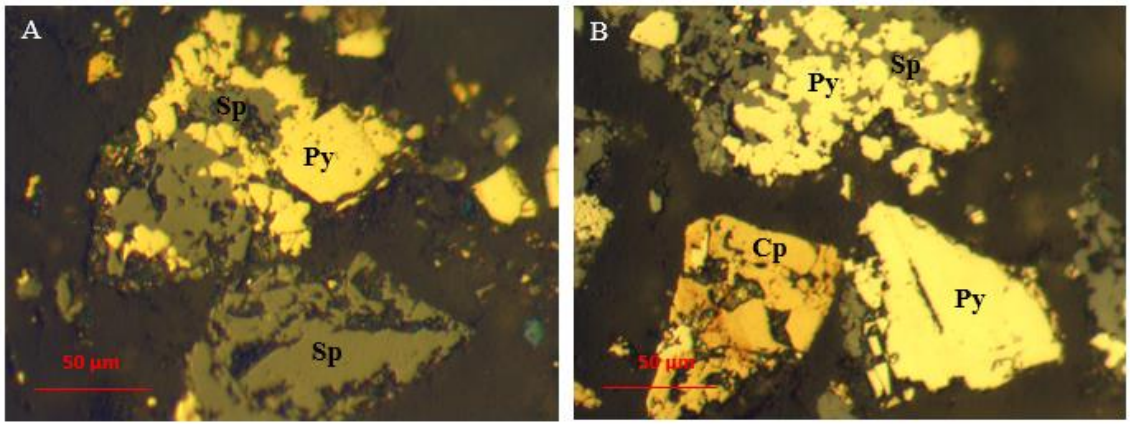

Figure 4: Micrographs: Sphalerite partially occluded in a pyrite particle (A) and chalcopyrite particle and sphalerite disseminated in a pyrite particle (B).

2.2 Leaching procedure

Ferric leaching experiments were carried out in a cylindrical 3L-reactor, with mechanical agitation fixed to 600 rpm, 3 deflectors and a heat exchanger connected to a thermostat. Leaching liquors were prepared from a commercial ferric solution (210 g/L Fe^{3+}), sulphuric acid solution (95% wt) and distilled water. Leaching dissolution was heated to the experimental temperature and later a determined mass of concentrate, previously magnetically shaken with a minimum amount of distilled water, is added. At selected time intervals, samples of a known volume were withdrawn and filtered. Zn^{2+}, Fe^{2+} and Fe_{total} on liquid fraction were measured. Zn^{2+} was measured by AAS, Perkin Elmer 2380 model, and Fe^{2+} and Fe_{total} were measured by redox titration with $K_2Cr_2O_7$. For Fe_{total} determination, a previous step of reduction with $SnCl_2$ was performed. From solid residue, weight loss was calculated and Zn, Cu, Pb and Ag concentration was analysed by AAS, previous acid digestion.

2.3 Kinetic model adjustment

Kinetic equations shown in Table 1 are fit to experimental data of different tests with the aim of confirming the kinetic model that estimates better the sphalerite leaching. The interpretation of kinetic models is discussed more fully in Dickinson and Heal (1999), Órfao and Martins (2002), Levenspiel (2004) and Khawam and Flanagan (2006).

In order to compare kinetic parameters obtained from different kinetic models, the initial rate of sphalerite dissolution is determined through the fitting of experimental data to a hyperbolic equation (eq. 1). This approach has been utilized by Souza et al. (2007a).

$$[Zn^{2+}] = \frac{k_1 \cdot t}{k_2 + t} \quad \text{(eq. 1)}$$

Where $[Zn^{2+}]$ = zinc concentration, t = time, k_1 and k_2 = constants. The initial leaching rate is the slope of eq. 1, at t = 0. That means the ratio between k_1 and k_2 ($k_1/k_2 = K$), since the first derivate of eq. 1 is eq. 2:

$$\frac{d[Zn^{2+}]}{dt} = \frac{k_1 \cdot k_2}{(k_2 + t)^2} \xrightarrow{t=0} \frac{d[Zn^{2+}]}{dt} = \frac{k_1}{k_2} = K \quad \text{(eq. 2)}$$

And for all purposes, K can be written as $K = A \cdot k_0 \cdot [Fe^{3+}]^n$, where A = reaction area, k_0 = Arrhenius constant, $[Fe^{3+}]$ = ferric ion concentration and n = order of reaction.

Hyperbolic equation adjustment to experimental data is carried out with MATLAB 2017a software, using the Levenberg-Marquardt algorithm, where eq.3 is minimised, being $[Zn^{2+}{}_{theo}]$ the zinc concentration obtained from eq. 1.

$$Q = \sum_k ([Zn^{2+}]_{exp,k} - [Zn^{2+}]_{theo,k})^2 \quad \text{(eq. 3)}$$

R^2 is obtained according to eq. 4, where $[Zn^{2+}]_{theo,ave,k}$ is the mean value of $Zn^{2+}{}_{theo}$ in data set.

$$R^2 = \frac{\sum_k \left([Zn^{2+}]_{exp,k} - [Zn^{2+}]_{theo,k}\right)^2}{\sum_k \left([Zn^{2+}]_{exp,k} - [Zn^{2+}]_{theo,ave,k}\right)^2} \quad \text{(eq. 4)}$$

3. Results and discussion

3.1 Effect of Variables

3.1.1 Effect of pulp density

Table 4 shows a summary of experiments carried out at different pulp densities (0.5-3%). In these experiments an increase of pulp density enhances the Zn extraction, because ferric ion concentration is not a limiting reagent. These results are according to Markus et al. (2004). Other authors (Dutrizac, 2006; Santos et al., 2010) observed a negative effect of an increase of the pulp density (upper than 5%) in batch experiments due to the depletion of ferric ion. Also, the increase of pulp density decreases the ratio final concentration of ferrous iron per mass of concentrate, due to the diminution of the dissolution rate of pyrite, as this sulphide has the higher rest potential. The decrease in weight loss when the pulp density increases also supports a lower pyrite dissolution rate.

Table 4: Results of experiments carried out with different pulp densities (0.36M Fe^{3+}, 0.2M H_2SO_4, Cl-B and 60 ºC).

Pulp density (%)	Zn extraction (%)	Weight loss (%)	Fe^{2+} final (mol/L)	Fe^{2+} final/concentrate mass ($1 \cdot 10^{-3} \cdot molL^{-1}g^{-1}$)
0.5	51.8	28.51	0.045	3.02
1.5	56.9	17.76	0.046	1.02
3.0	62.3	15.33	0.090	0.99

3.1.2 Effect of ferric ion concentration

Ferric ion is directly involved in sphalerite leaching reaction, so it is expected an important role of ferric ion in reaction rate. Table 5 shows the results obtained with different ferric ion concentrations, where it can be observed that an increase of ferric ion concentration gradually enhances the sphalerite dissolution, these results are consistent with those obtained by Salmi et al. (2010), Dutrizac (2006), Markus et al. (2004) and Souza et al. (2007a).

Table 5: Results of experiments carried out at different ferric ion concentrations (0.5% pulp density, 0.2M H_2SO_4, Cl-B and 60 ºC).

Initial ferric ion (mol/L)	Zn extraction (%)	Weight loss (%)	Fe^{2+} final ($1 \cdot 10^{-3}$ mol/L)	Fe^{2+} final / mass concentrate ($1 \cdot 10^{-3} \cdot molL^{-1}g^{-1}$)
0.18	47.9	21.39	38	2.51
0.36	51.8	28.51	45	3.02
0.72	71.0	29.13	69.7	4.65

3.1.3 Effect of sulphuric acid concentration

Table 6 shows a summary of results obtained from experiments at different sulphuric acid concentrations, it seems that these results have not dependence with the initial sulphuric acid concentration. This is according to Salmi et al. (2010) and Santos et al. (2010). Also, the ratio between $Fe^{2+}{}_{final}$ and mass of concentrate shows that no sulphide, in this bulk concentrate, is affected by sulphuric acid concentration.

Table 6: Results of experiments with different sulphuric acid concentrations (0.36M Fe^{3+}, 0.5% pulp density, Cl-B and 60 ºC).

Initial sulphuric acid (mol/L)	Zn extraction (%)	Weight loss (%)	Fe^{2+} final (10^{-3} mol/L)	Fe^{2+} final / mass concentrate (10^{-3}·molL^{-1}g^{-1})
0.20	51.8	28.51	45	3.02
0.51	51.9	28.45	45	3.01
1.02	52.5	28.50	46	3.06

3.1.4 Effect of ferrous and sulphate ions concentration

In all leaching commercial processes there is an initial ferrous concentration, as during the leaching process ferric ion is reduced to ferrous ion (Dutrizac, 2006). Therefore, it is important to know the influence of ferrous ion concentration on sphalerite oxidation kinetics. This possible dependence may be due to a decrease of redox potential, according to the electrochemical model proposed by Verbaan and Crundwell (1986), or to an increase of initial sulphate concentration. To determinate how the addition of ferrous sulphate concentration can affect the process rate, some experiments at different initial $FeSO_4$ and $MgSO_4$ concentrations (0-0.36M) are carried out. Fig. 5 shows Zn extraction as a function of the time for different concentrations of ferrous sulphate (A) and of magnesium sulphate (B) concentrations. In both cases, the presence of an initial concentration of Fe^{2+} or SO_4^{2-} (until 0.36M) have no influence on sphalerite dissolution rate. The lack of this influence would be advantageous in the continuous operation.

These results are not in concordance with those obtained by Dutrizac (2006), where a dependence between the process rate and the initial ferrous sulphate concentration was found, other references about these observations have not been found in literature.

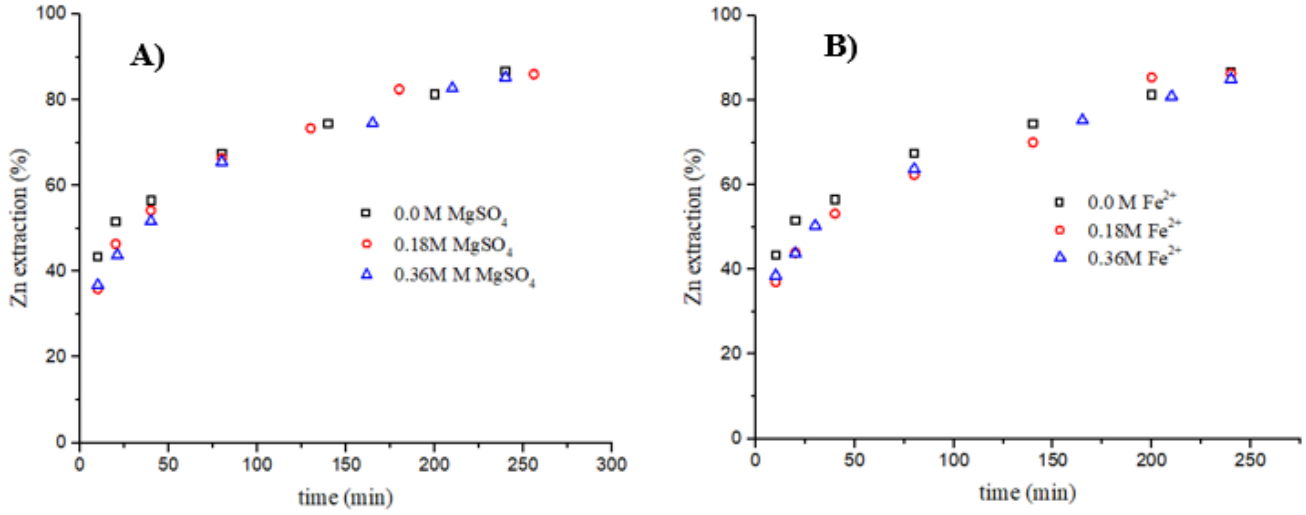

Figure 5: Effect of ferrous ion (A) and sulphate (B) concentrations on Zn extraction (0.54M Fe^{3+}, 2% pulp density, 80 ºC and bulk concentrate).

3.1.5 Effect of particle size

Particle size plays a key role in sulphide dissolution reactions. Dutrizac (2006) and Da Silva (2004) observed a notorious effect in the dissolution rate when particle size decreased. In return, Souza et al. (2007a) did not observe this effect with a minor particle size, due to a similar surface area in all particle sizes fractions, as samples with a higher particle size shown a greater porosity. In Fig. 6A it can be observed that a decrease of particle size substantially enhances the sphalerite dissolution rate. The decrease of the particle size also has a great influence on the dissolution of other sulphides. In Table 7 the final ferrous ion concentration and the weight loss of different experiments are shown.

Table 7: Ferrous ion concentration and weight loss measured in experiments at different particle sizes.

Sample	D80 (µm)	Fe^{2+}final (10^{-3} mol/L)	Weight loss (%)
Cl-A	43.7	34	20.05
Cl-B	14.8	45	28.51
Cl-C	10.2	54	30.71

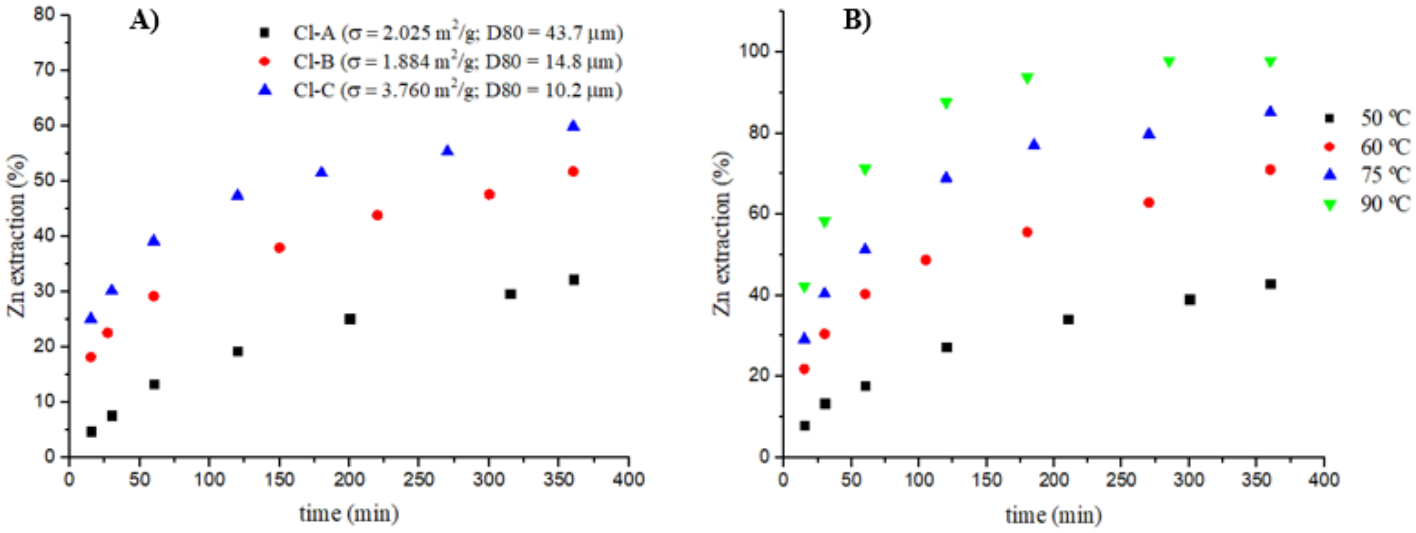

Figure 6: Zn extraction as a function of time and particle size (A) (0.36M Fe^{3+}, 0.2M H_2SO_4, 0.5% pulp density and 60 ºC); Zn extraction as a function of time and temperature (B) (0.72M Fe^{3+}, 0.2M H_2SO_4, 0.5% pulp density and Cl-B).

3.1.6 Effect of temperature

Fig. 6B shows the evolution of zinc extraction when Cl-B is leached at different temperatures, in the range of 50-90 ºC. Similar results were observed by Dutrizac (2006), Souza et al. (2007a), Salmi et al. (2010), Palencia et al. (1990) and Markus et al. (2004). At 50 ºC Zn extraction is lower than 40% in 6 hours. However, an increment of temperature to 90 ºC enhances Zn extraction to 97.9% in 4.75 hours. The rest of sulphides are also dissolved at a higher rate when temperature is increased, inasmuch of at the end of the experiments ferrous ion concentrations, that is directly related with the sulphides dissolution, varies from 0.04M at 50 ºC to 0.15M at 90 ºC.

3.1.7 Effect of elemental sulphur film

Many authors (Da Silva, 2004; Souza et al., 2007a; Crundwell, 1987a; Chang et al., 1994; Lochman and Pedlík, 1995) observed a key role of elemental sulphur in sphalerite oxidation kinetic. Elemental sulphur forms a non-porous film around sphalerite particle that hinders the ferric ion transport from solution to mineral surface. SEM images of leaching residues obtained by Souza et al. (2007a) show a progressive increase in the amount of elemental sulphur covering the particle surfaces, after 45% zinc extraction the particles present their surface completely covered by an elemental sulphur layer.

With the aim to determinate the effect of elemental sulphur layer, two experiments with the same experimental conditions are performed. In one of them, after 30 min of reaction, the pulp is filtered and the elemental sulphur is removed from the solid with CS_2, later the concentrate without S^0 is added into the leaching solution recuperated after filtration. In Fig. 7 it can be seen that after elemental sulphur removal, the process rate does not suffer a deceleration. Therefore, elemental sulphur plays an important role in sphalerite leaching process, limiting reaction rate to diffusion through a non-porous film.

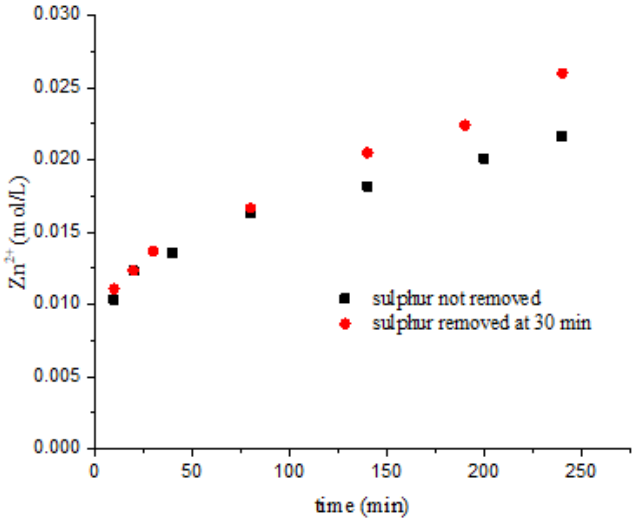

Figure 7: Effect of elemental sulphur film on Zn^{2+} concentration as a function of time (0.54M Fe^{3+}, 0.2M H_2SO_4, 2% pulp density, 80 ºC and global concentrate).

3.2 Kinetic analysis

A non-acceptable linear relationship is obtained when kinetic model are fit to the set of experimental data. Models with diffusion as the rate controlling step have a R^2 higher than 0.93 in all cases, but the early experimental data are deviated always above the values predicted by the models. As long as model with chemical control only have a linear relationship with data at short reaction times.

Two kinetic regimes are proposed in view of these observations. A first stage, where the process rate is the maximum and the rate controlling step is the chemical reaction on sphalerite surface; and a second stage where the rate decreases due to a passivating film formation that changes the rate controlling step to the diffusion through an elemental sulphur layer. This change of mechanism is produced around 30% Zn extraction. The hypothesis of two kinetic regimes is according to Souza et al. (2007a), Lochman and Pedlik (1995); Weisener et al. (2003), Crundweel (1987b) and Karimi et al. (2017). Also,

Da Silva (2004), and Bobeck and Su (1985) observed a mixed control (chemical and diffusion).

Models F1, F2 and R3 are the models with the best linear relationship at the first stage, and the models D3, D4, D5 and D8 have a good linear fit to the second stage. The model D8 supposes a cylindrical geometry with a slight surface area, therefore this model is discarded to explain the reaction in a rough bulk concentrate. To check the kinetics parameters obtained from the kinetic model applied in the first stage, where the experimental data is limited, the initial rate of different tests is calculated. Fig. 8A shows the fit of hyperbolic equation (initial rate) to experimental data at different temperatures.

In order to observe which model estimates better the sphalerite dissolution reaction, the kinetic parameters are calculated from the different models and from the initial rate determination. In Table 8 the estimation of the kinetic parameters is shown.

Table 8: Kinetic parameters estimation from different models (Fe^{3+} = reaction order with respect ferric ion; ZnS = dependence on sphalerite amount in the process rate; Ea = Apparent activation energy; IR = initial rate).

	Chemical stage				**Diffusional stage**		
Model	**F1**	**R3**	**F2**	**IR**	**D3**	**D4**	**D5**
R^2	0.939	0.932	0.957	0.981	0.984	0.977	0.981
Ea (kJ/mol)	51.3 ± 11.5	38.7 ± 8.3	49.6 ± 8.6	50.7 ± 10.1	67.6 ± 10.3	47.7 ± 9.8	131.0 ± 17.0
Fe^{3+}	0.26 ± 0.04	0.25 ± 0.03	0.30 ± 0.06	0.203 ± 0.002	1	1	1
ZnS	1	2/3	2	1.08 ± 0.11	2/3	1/3	5/3

Kinetic parameters, for chemical stage, from model F1 are those that have a greater similarity with respect IR determination, this is according to Markus et al. (2004) and Salmi et al. (2010), where the reaction rate is proportional to available sphalerite, contained in a rough and porous solid. The activation energies and the reaction order with respect ferric ion obtained from different models are similar in all cases.

In the second stage, models D3-D5 have a high value of R^2, but the apparent activation energies estimated for each model oscillate from 47.7 to 131.0 kJ/mol, the lower value, corresponding to model D4, is the most similar with the values obtained in the first stage.

Fig. 8B shows as model F1 is adjusted to early experimental data and about 30% Zn extraction experimental data is fit to model D4.

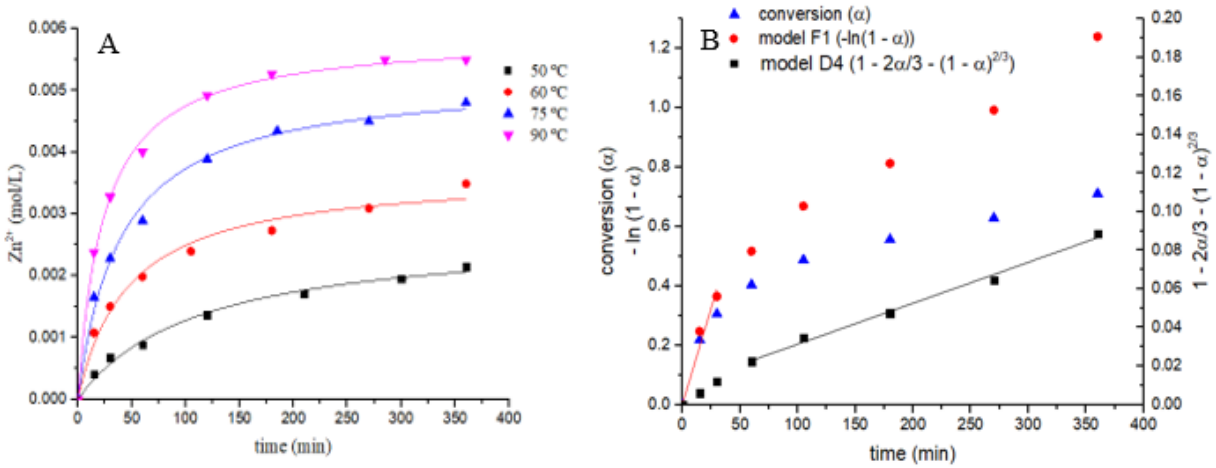

Figure 8: Fit of hyperbolic equation to experimental data at different temperatures (0.72M Fe^{3+}, 0.2M H_2SO_4, 0.5% pulp density and Cl-B sample) (A) and fit of the model F1 in the first stage and the model D4 in the second stage (0.72M Fe^{3+}, 0.2M H_2SO_4, 0.5% pulp density, Cl-B and 60 ºC) (B).

Kinetic parameters of sphalerite leaching reaction with ferric sulphate of the two kinetic regimes are estimated from model F1, model D4 and the IR. Two different apparent activation energies are observed for the different kinetic regimes. The activation energy of the chemical stage is 51.3 kJ/mol (model F1) that corresponds with the activation energy of the chemical reaction on the sphalerite surface, this value is similar to Ea calculated from IR (50.7 kJ/mol) because at the beginning of the reaction the rate controlling step is the chemical reaction, supporting the chemical control at early reaction time. The apparent activation energy for the diffusional stage (47.7 kJ/mol) is lower than for the first stage, as the rate controlling step is the diffusion. This activation energy is high for a diffusionally controlled process, with a typical value about 12.6 kJ/mol, but in a mixed process, the activation energy can be similar to processes with a chemical control (Bobeck and Su, 1985). Table 9 presents several values of activation energies obtained from various studies, the values obtained in this work are according to most of them.

Table 9: Activation energies, obtained in other studies, to different sphalerite samples.

Activation energy (kJ/mol)	Model applied	System	Reference
46,9 ± 11,3	Mixed control	$FeCl_3$	(Bobeck and Su, 1985)
34 ± 4	Differential method	O_2	(Weisener et al., 2003)
44	Chemical control	$Fe_2(SO_4)_3$	(Dutrizac, 2006)
41± 2	Diffusional control	$K_2S_2O_8$	(Babu et al, 2002)
58,4	Chemical control	$FeCl_3$	(Jin et al., 1984)
27,5 (chemical) 19,6 (diffusion)	Mixed control	$Fe_2(SO_4)_3$	(Souza et al., 2007a)
53,2	Chemical control	$Fe_2(SO_4)_3$	(Salmi et al, 2010)
67	Chemical control	$Fe_2(SO_4)_3$	(Markus et al, 2004)
75,2 (50-70 ºC) 20,3 (70-90 ºC)	Diffusional control	$Fe_2(SO_4)_3$	(Palencia et al., 1990)
70 (0,04% Fe) 40 (12,5% Fe)	Chemical control	$Fe_2(SO_4)_3 – FeCl_3$	(Palencia and Dutrizac, 1991)

The reaction order calculated for ferric ion is 0.26, a low value that supports a chemical control at the beginning of the reaction, as the diffusional control order expected with respect to liquid phase is 1. Other authors found an order of 0.34 (100 ºC) and 0.39 (75 ºC) with respect to ferric ion, as $Fe_2(SO_4)_3$, (Dutrizac, 2006), and a value of 0.36 with respect ferric ion, as $FeCl_3$, (Dutrizac and Macdonald, 1978), applying kinetic models with chemical control.

Concentration of solid reagent is not usually a meaningful term in solid state reaction. However, the reaction rate depends on the reaction surface area, and this depends on the sphalerite amount. It is expected that the process rate is proportional to the sphalerite amount in a concentrate with a high specific surface area, according to eqs. 5-7. Eq. 6 defines the shape factor (a) as the relation between accessible surface area and particle volume, and the eq. 7 relates the reaction surface area (A) with the shape factor (a), the solid molar mass (M), the initial molar fraction (x_{oi}), the initial sphalerite amount (n_{0i}) and the sphalerite amount (n_i). When σ is high, the value of 1 – 1/a is close to 1, that is the value observed in this work, and it is according to Markus et al. (2004) and Salmi et al. (2010).

$$\frac{dZn^{2+}}{dt} = \upsilon_{Zn^{2+}} \cdot r \cdot A \qquad \text{(eq. 5)}$$

$$a = \frac{A_p}{V_p} r_0 = \rho r_0 \sigma \qquad \text{(eq. 6)}$$

$$A = \frac{\sigma M}{x_{0i}} n_{0i}^{1/a} n_i^{1-1/a} \xrightarrow{a \gg 3} A = \frac{\sigma M}{x_{0i}} n_i \qquad \text{(eq. 7)}$$

The values of k for model F1, obtained with different particle sizes, show a linear relationship with respect to $1/r_0$ and 1/D80 (μm^{-1}). The k values of the model D4, in the diffusional stage, fit a linear relationship with respect to $1/r_0^2$ and $1/D80^2$ (μm^{-2}). Fig. 9 presents these linear relationships, supporting the assumption of an initial chemical control and later a diffusional control.

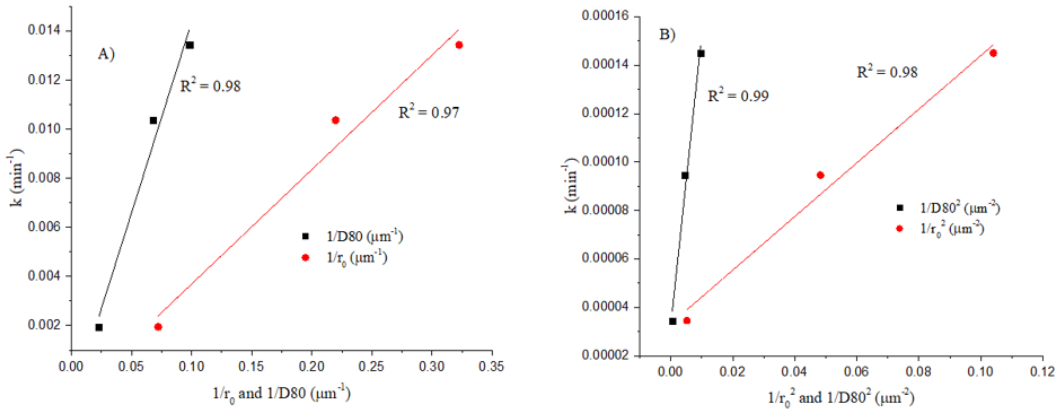

Figure 9: Linear fit between $1/r_0$, and1/D80, and k for model F1 (A) and between $1/r_0^2$, and $1/D80^2$, and k for model D4 (B).

In the same way, Fig. 10 shows the representation of surface area of the bulk concentrate versus K (IR) at different particle sizes and pulp densities, where the surface area increases according to eq. 7. Theoretically, K (IR) is proportional to sphalerite surface area, but in this case only the surface area of the bulk concentrate (A) is known, being K = 0 when A = 0. Only the samples with a particle size minor than 25 µm follow a linear relationship between surface area and K, so that in these samples the sphalerite surface area can be considered proportional to the surface area of the bulk concentrate. This observation suggests that a part of sphalerite in Cl-A (> 25 µm) is occluded in pyrite matrix, which hinder the access of leaching liquor to sphalerite particles, that is according to the micrographs shown in Fig. 4. This could be a pivotal factor, because greatly affects the sphalerite dissolution rate. Therefore, it should be considered in the design of a

hydrometallurgical process, where the majority sulphide is pyrite, and in large particles of pyrite a part of non-ferrous sulphides can be encapsulated.

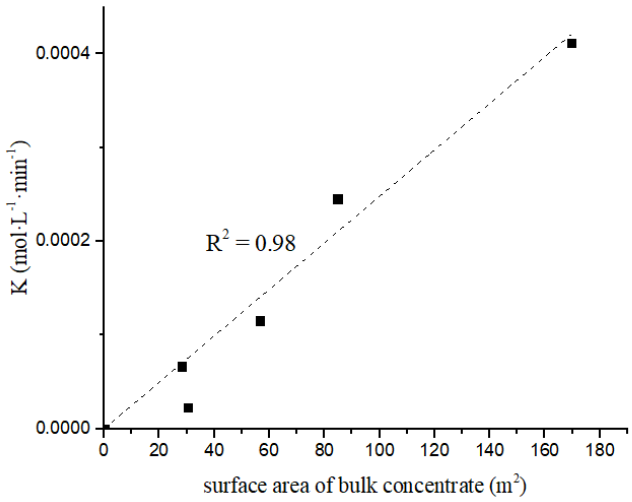

Figure 10: Surface area (m^2) vs K ($mol \cdot L^{-1} \cdot min^{-1}$), linear fit excluding sample Cl-A (0.32M Fe^{3+}, 0.20M H_2SO_4, 60 ºC).

3.2 Leaching solid residue

Solid residues obtained after ferric leaching have the mean composition in Cu, Pb and Ag shown in Table 10, copper is found as chalcopyrite and lead as anglesite ($PbSO_4$). This residue is susceptible to be treated through other hydrometallurgical processes to benefit the target metals. Within the framework of the project described above, the following leaching stages are a silver-catalysed ferric leaching, where Cu is dissolved, and a brine leaching to dissolve Pb and Ag (contained in the concentrate and added as catalyst), such as it is shown in Fig. 1. Results of the catalysed ferric leaching and the brine leaching are expected to be published in forthcoming papers.

Table 10: Mean composition and standard deviation in valuable compounds of solid residue.

Compound	Cu (%)	Pb (%)	Ag (ppm)	$CuFeS_2$ (%)	$PbSO_4$ (%)
Mean value	5.01	5.76	116	14.47	8.43
Standard deviation	0.86	2.07	42	2.48	3.03

4. Conclusions

The kinetics of the sphalerite dissolution contained in a bulk concentrate with ferric sulphate is studied for the first time. Only the variables that are directly involved in the oxidative dissolution of sphalerite play a key role in the leaching rate (Ferric ion, Temperature and particle size). The addition of sulphuric acid (0.2-1.0 M), ferric sulphate (0-0.36 M) and magnesium sulphate (0-0.36 M) have no influence on the reaction rate. When the elemental sulphur is removed from partially leached solid, the reaction rate does not suffer a deceleration at long reaction times.

At the beginning of reaction, experimental data fits a first order-kinetics to solid particle model (F1), where the rate controlling step is the chemical reaction on the sphalerite surface. At 30% Zn extraction, experimental data is deviated from model F1 and is fit to model D4, possibly due to the formation of a non-porous film of elemental sulphur.

The estimated activation energy of the chemical reaction has a value of 51.3 kJ/mol. When the diffusion is the rate controlling step, the second stage, the apparent activation energy is 47.7 kJ/mol. Order-kinetics to ferric ion is 0.26 and 1 in the chemical and the diffusional stage, respectively. The process rate is proportional to the sphalerite amount. When samples are lesser than 25 µm, the reaction rate is proportional to surface area of bulk concentrate, because at higher particle sizes part of the sphalerite is occluded.

These results evidence that the ferric leaching of sphalerite in the presence of other sulphides has a similar behaviour to that of the high-grade sphalerite. These observations show the possibility to obtain Zn from a bulk concentrate and enable the treatment of the solid leaching residue through a hydrometallurgical process to extract the rest of valuable metals, in this case Cu, Pb and Ag.

5. Acknowledgements

Authors appreciate the financial support of CLC Company (PRJ201602665/0124).

AGQ Mining & Bioenergy and CLC supplied the samples of the bulk concentrate.

6. Bibliography

Aydogan, S., Aras, A., Canbazoglu, M. (2005). Dissolution kinetics of sphalerite in acidic ferric chloride leaching. Chemical Engineering Journal 114, 67–72.

Babu, M. N., Sahu, K. K., & Pandey, B. D. (2002). Zinc recovery from sphalerite concentrate by direct oxidative leaching with ammonium, sodium and potassium persulphates. Hydrometallurgy, 64(2), 119-129.

Bahram, B., & Javad, M. (2011). Chloride leaching of lead and silver from refractory zinc plant residue. Research Journal of Chemistry and Environment, Vol, 15, 2.

Barriga Mateos, F., Pereda Marin, J., Palencia Perez, I. (1993). Bacterial leaching of a bulk flotation concentrate of chalcopyrite – sphalerite. Biorecovery 2, 195 – 218.

Bobeck, G., & Su, H. (1985). The kinetics of dissolution of sphalerite in ferric chloride solution. Metallurgical transactions B, 16(3), 413-424.

Brown, M. E., Dollimore, D., & Galwey, A. K. (1980). Reactions in the Solid State, vol. 22 of Comprehensive Chemical Kinetics, Bamford, CH and Tipper, CFH, Eds.

Carranza, F. (1985). Las piritas españolas: un recurso natural poco explotado. Quím, Sur. Jul. 13-15.

Carranza, F., Iglesias, N., Romero, R., & Palencia, I. (1993). Kinetics improvement of high-grade sulphides bioleaching by effects separation. FEMS microbiology reviews, 11(1-3), 129-138.

Carranza, F., Palencia, I., & Romero, R. (1997a). Silver catalyzed IBES process: application to a Spanish copper-zinc sulphide concentrate. Hydrometallurgy, 44(1-2), 29-42.

Carranza, F., Palencia, I., Romero, R., Iglesias, N. (1997b). Application fields of the BRISA process. Influence of the ore mineralogy on the process flowsheet. In: Australian Mineral Foundation (Eds.), Proceedings of the International Biohydrometallurgy Symposium IBS97-BIOMINE 97 ‘‘Biotechnology Comes of Age’’, Sydney, Australia, 4 – 6 August, 1997. Australian Mineral Foundation, pp. M2.1.1 –M2.1.10.

Carranza, F., Iglesias, N., Mazuelos, A., Palencia, I., & Romero, R. (2004). Treatment of copper concentrates containing chalcopyrite and non-ferrous sulphides by the BRISA process. Hydrometallurgy, 71(3), 413-420.

Chang, C. Y., Clarkson, C. J., & Manlapig, E. V. (1994, December). The leaching of zinc sulphide concentrate in sulphate-chloride solutions with ferric ions. In AusIMM Proceedings(Australia) (Vol. 299, No. 2, pp. 57-62).

Conic, V. T., Vujasinovic, M. M. R., Trujic, V. K., & Cvetkovski, V. B. (2014). Copper, zinc, and iron bioleaching from polymetallic sulphide concentrate. Transactions of Nonferrous Metals Society of China, 24(11), 3688-3695.

Córdoba, E. M., Muñoz, J. A., Blázquez, M. L., González, F., & Ballester, A. (2008). Leaching of chalcopyrite with ferric ion. Part I: General aspects. Hydrometallurgy, 93(3), 81-87.

Crundwell, F. K. (1987a). Refractory behaviour of two sphalerite concentrates to dissolution in ferric sulphate solutions. Hydrometallurgy, 19(2), 253-258.

Crundwell, F. K. (1987b). Kinetics and mechanism of the oxidative dissolution of a zinc sulphide concentrate in ferric sulphate solutions. Hydrometallurgy, 19(2), 227-242.

Crundwell, F. K. (1988). Effect of iron impurity in zinc sulfide concentrates on the rate of dissolution. AIChE journal, 34(7), 1128-1134.

Da Silva, G., Lastra, M. R., & Budden, J. R. (2003). Electrochemical passivation of sphalerite during bacterial oxidation in the presence of galena. Minerals Engineering, 16(3), 199-203.

Da Silva, G. (2004). Relative importance of diffusion and reaction control during the bacterial and ferric sulphate leaching of zinc sulphide. Hydrometallurgy, 73(3), 313-324.

Deller, G. (2005). World zinc supply and demand-heading for a late-decade price spike. Lead & zinc, 5, 17-25.

Dickinson, C. F., & Heal, G. R. (1999). Solid–liquid diffusion controlled rate equations. Thermochimica Acta, 340, 89-103.

Dutrizac, J. E. (2006). The dissolution of sphalerite in ferric sulfate media. Metallurgical and Materials Transactions B, 37(2), 161-171.

Dutrizac, J. E., & MacDonald, R. J. C. (1978). The dissolution of sphalerite in ferric chloride solutions. Metallurgical Transactions B, 9(4), 543-551.

Dutrizac, J.E., Pratt, A.R., Chen, T.T. (2003). The mechanism of sphalerite dissolution in ferric sulphate–sulphuric acid media. In: Yazawa International Symposium, Metallurgical and Materials Processing: Principles and Technologies, Aqueous and Electrochemical processing. Vol. III, pp. 139-161.

Elsherief, A. E. (1994). Influence of galvanic interactions between chalcocite and sphalerite during the early stage of leaching. Minerals Engineering, 7(11), 1387-1399.

Estrada-de los Santos, F., Rivera-Santillán, R. E., Talavera-Ortega, M., & Bautista, F. (2016). Catalytic and galvanic effects of pyrite on ferric leaching of sphalerite. Hydrometallurgy, 163, 167-175.

Ghahremaninezhad, A., Radzinski, R., Gheorghiu, T., Dixon, D. G., & Asselin, E. (2015). A model for silver ion catalysis of chalcopyrite ($CuFeS_2$) dissolution. Hydrometallurgy, 155, 95-104.

Gomez, C., Blazquez, M. L., & Ballester, A. (1999). Bioleaching of a Spanish complex sulphide ore bulk concentrate. Minerals Engineering, 12(1), 93-106.

Gomez, C., Limpo, J. L., De Luis, A., Blazquez, M. L., Gonzalez, F., & Ballester, A. (1997). Hydrometallurgy of bulk concentrates of Spanish complex sulphides: Chemical and bacterial leaching. Canadian metallurgical quarterly, 36(1), 15-23.

Grénman, H., Salmi, T., & Murzin, D. Y. (2011). Solid-liquid reaction kinetics–experimental aspects and model development. Reviews in Chemical Engineering, 27(1-2), 53-77.

Habashi, F. (2005). A short history of hydrometallurgy. Hydrometallurgy, 79(1), 15-22.

Haghshenas, D. F., Bonakdarpour, B., Alamdari, E. K., & Nasernejad, B. (2012). Optimization of physicochemical parameters for bioleaching of sphalerite by Acidithiobacillus ferrooxidans using shaking bioreactors. Hydrometallurgy, 111, 22-28.

Jin, Z. M., Warren, G. W., & Henein, H. (1984). Reaction kinetics of the ferric chloride leaching of sphalerite—an experimental study. Metallurgical transactions B, 15(1), 5-12.

Karimi, S., Rashchi, F., & Moghaddam, J. (2017). Parameters optimization and kinetics of direct atmospheric leaching of Angouran sphalerite. International Journal of Mineral Processing, 162, 58-68.

Khawam, A., & Flanagan, D. R. (2006). Solid-state kinetic models: basics and mathematical fundamentals. The journal of physical chemistry B, 110(35), 17315-17328.

Lampinen, M., Laari, A., & Turunen, I. (2015). Kinetic model for direct leaching of zinc sulfide concentrates at high slurry and solute concentration. Hydrometallurgy, 153, 160-169.

Levenspiel, O. (2004). Chemical Engineering Reactions. New York. Jonh Wiley & Sons.

Lizama, H. M., Fairweather, M. J., Dai, Z., & Allegretto, T. D. (2003). How does bioleaching start?. Hydrometallurgy, 69(1), 109-116.

Lo, W. W., Surges, L. J., & Hancock, H. (1985). The Preferential Aqueous Oxidation of Sphalerite in a Mixed Sulphide Tailing Using Manganese Dioxide. Complex Sulfides--Processing of Ores, Concentrates and By-Products, 907-923.

Lochmann, J., & Pedĺik, M. (1995). Kinetic anomalies of dissolution of sphalerite in ferric sulfate solution. Hydrometallurgy, 37(1), 89-96.

Majima, H. (1969). How oxidation affects selective flotation of complex sulphide ores. Canadian Metallurgical Quarterly, 8(3), 269-273.

Markus, H., Fugleberg, S., Valtakari, D., Salmi, T., Murzin, D. Y., & Lahtinen, M. (2004). Kinetic modelling of a solid–liquid reaction: reduction of ferric iron to ferrous iron with zinc sulphide. Chemical Engineering Science, 59(4), 919-930.

Mazuelos, A., Carranza, F., Palencia, I., & Romero, R. (2000). High efficiency reactor for the biooxidation of ferrous iron. Hydrometallurgy, 58(3), 269-275.

Mehta, A.P., Murr, L.E., 1982: Kinetic study f sulphide leaching by galvanic interaction between chalcopyrite, pyrite, and sphalerite in the presence of T. ferrooxidans (30 ºC) and a thermophilic microorganism (55 ºC). Biotechnol. Bioeng. 24, 919-940.

Mizoguchi, T., & Habashi, F. (1983). Aqueous oxidation of zinc-sulphide, pyrite and their mixtrues in hydrochloric-acid. Transactions of the institution of mining and metallurgy section c-mineral processing and extractive metallurgy, 92(MAR), C14-C19.

Orfao, J. J. M., & Martins, F. G. (2002). Kinetic analysis of thermogravimetric data obtained under linear temperature programming—a method based on calculations of the temperature integral by interpolation. Thermochimica Acta, 390(1), 195-211.

Ortega, A., & Bonilla, A. (1983). Flotación de sulfuros complejos de matriz pirítica. Estudio de posibilidades de tratamiento de sus concentrados. In Anales del III Congreso Nacional de Metalurgia, Santiago de Chile (Vol. 280).

Palencia, I., Carranza, F., & Garcia, M. J. (1990). Leaching of a copper-zinc bulk sulphide concentrate using an aqueous ferric sulphate dilute solution in a semicontinuous system. Kinetics of dissolution of zinc. Hydrometallurgy, 23(2-3), 191-202.

Palencia I. & Dutrizac, J. E. (1991). The effect of the iron content of sphalerite on its rate of dissolution in ferric sulphate and ferric chloride media. Hydrometallurgy, 26(2), 211-232.

Palencia, I.; Romero, R.; Carranza, F. Silver catalyzed IBES process: application to a Spanish copper–zinc sulphide concentrate. Part 2. Biooxidation of the ferrous iron and catalyst recovery. Hydrometallurgy, 1998, vol. 48, no 1, p. 101-112.

Salmi, T., Grénman, H., Bernas, H., Wärnå, J., & Murzin, D. Y. (2010). Mechanistic modelling of kinetics and mass transfer for a solid–liquid system: Leaching of zinc with ferric iron. Chemical Engineering Science, 65(15), 4460-4471.

Santos, S. M., Machado, R. M., Correia, M. J. N., Reis, M. T. A., Ismael, M. R. C., & Carvalho, J. M. (2010). Ferric sulphate/chloride leaching of zinc and minor elements from a sphalerite concentrate. Minerals Engineering, 23(8), 606-615.

Souza, A. D. D., Pina, P. D. S., Leão, V. A., Silva, C. A. D., & Siqueira, P. D. F. (2007a). The leaching kinetics of a zinc sulphide concentrate in acid ferric sulphate. Hydrometallurgy, 89(1), 72-81.

Souza, A. D., Pina, P.S., Leao, V.A., (2007b). Bioleaching and chemical leaching as an integrated process in the zinc industry. Minerals Engineering 20 (6), 591-599.

Tipre, D. R., & Dave, S. R. (2004). Bioleaching process for Cu–Pb–Zn bulk concentrate at high pulp density. Hydrometallurgy, 75(1), 37-43.

Tipre, D.R., Vora, S.B., Dave, S.R. (1999). Comparative copper and zinc bioextraction at various stages of scale up using Thiobacillus ferrooxidans consortium. In: Amils, R., Ballester, A. (Eds.), Proc. International Biohydrometallurgy Symposium on Biohydrometallurgy and the Environment towards the Mining of the 21st Century, Part A. Elsevier, Amsterdam, pp. 219 – 229.

Verbaan, B., & Crundwell, F. K. (1986). An electrochemical model for the leaching of a sphalerite concentrate. Hydrometallurgy, 16(3), 345-359.

Weisener, C. G., Smart, R. S. T. C., & Gerson, A. R. (2003). Kinetics and mechanisms of the leaching of low Fe sphalerite. Geochimica et Cosmochimica Acta, 67(5), 823-830.

Xu, B., Yang, Y., Li, Q., Jiang, T., & Li, G. (2016). Stage leaching of a complex polymetallic sulfide concentrate: focus on the extraction of Ag and Au. Hydrometallurgy, 159, 87-94.

Xu, B., Zhong, H., Wang, K. T., & Jiang, T. (2011). Two stage adverse current oxygen pressure acid leaching of complex Cu-Pb-Zn-Ag bulk concentrate. The Chinese Journal of Nonferrous Metals, 4, 029.